

Thermal Characteristics and Kinetic Parameters Assessment of Chitosan

Sevgi Polat^{1*}, Perviz Sayan¹

¹Marmara University, Faculty of Engineering, Department of Chemical Engineering, Istanbul, Turkey

*Corresponding author : sevgi.polat@marmara.edu.tr
Orcid No: 0000-0002-0934-2125

Abstract: In the present study, thermal decomposition kinetics of chitosan was investigated by a thermal analyzer. Firstly, the experiments were performed at three different heating rates from 30 °C to 800 °C under inert N₂ atmosphere. The results showed that the heating rate significantly affected the maximum peak temperature but it did not affect the conversion. When the heating rate increased, the maximum peak temperature shifted towards the higher temperature region. In the second part, the obtained thermal data was used to calculate the activation energies based on Flynn-Wall-Ozawa (FWO), Kissinger-Akahira-Sunose (KAS), Starink and Tang kinetic models. All models used provided accurate fits of experimental data and yielded acceptable errors. The values of the average activation energy for FWO, KAS, Starink and Tang models were determined to be 148.5, 146.4, 148.3 and 146.7 kJ/mol, respectively.

Keywords: Chitosan, Kinetics, Thermal decomposition, Model free

© EJBCS. All rights reserved.

1. Introduction

Chitosan is a natural polysaccharide biopolymer and it is widely used in the biotechnology, biomedicine, food, agriculture and cosmetics industries (Kast et al. 2002; Lozano-Navarro et al. 2018). The use of chitosan is generally preferred due to its widespread availability, hydrophilicity, biocompatibility, non-toxicity, cost effectiveness, antibacterial properties and immunostimulatory activities (Qu et al. 2000; Hamedi et al. 2018). Moreover, since chitosan is a kind of environment-friendly polymer material, its recycling in nature is often of primary interest to the scientific community, to understand its thermal decomposition. Its degradation in various environmental conditions causes to a destruction of chains by breaking, splitting of fragments of the main chain or side constituents and release of volatile products. The knowledge of its thermal kinetics may help better understanding and planning of its industrial processes because the adequate kinetic description of chemical and physical processes can be profitably applied for process design and optimization, and valid predictions (Zhou et al. 2009).

Thermogravimetric analysis (TGA) is one of the most common techniques, which allows obtaining reliable data to investigate thermal events and kinetics during decomposition of the materials. The kinetics of the thermal events have been determined by the application of the different kinetic models. Also, thermal decomposition in thermogravimetric analysis gives clues about the thermal

behaviors at different temperature regions for the decomposition process. In the current study, thermal decomposition of the chitosan was performed using the thermogravimetric analyzer. From the obtained TGA data, the kinetic parameter such as activation energy for the thermal decomposition process of the chitosan was calculated.

2. Materials and Method

Chitosan used in this study was provided from Sigma-Aldrich Chemical Company and was of reagent grade. Thermogravimetric analysis experiments were performed by using the Setaram Labsys Evo instrument. 10 ± 0.5 mg of the sample was taken in Al₂O₃ crucible and the measurements were performed under a constant N₂ flow rate of 25 cm³/min from 30 °C to 800 °C at heating rates of 5, 10 and 20 °C/min. The nitrogen flow ensured an inert atmosphere on the sample during the run, while the small amount of sample and the slow heating rate ensured that the heat transfer limitations can be ignored. From this analysis, thermogravimetric (TG) and differential thermogravimetric (DTG) curves were obtained and the experimental data was used to calculate the activation energy based on FWO, KAS, Starink, and Tang kinetic models.

3. Results and Discussion

3.1. TG/DTG Analysis

The TG and DTG curves obtained at different heating rates are shown in Figure 1. Based on these curves, two stages

can be observed during the thermal decomposition of the chitosan.

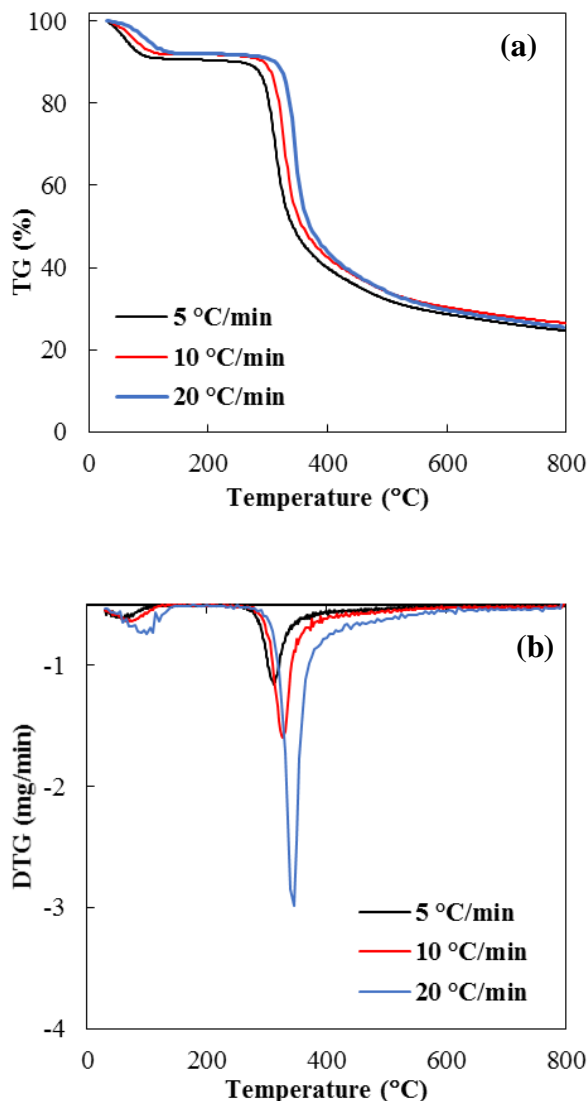


Figure 1. TG (a) and DTG (b) curves of chitosan at different heating rates

In the first stage occurring at temperature about 100 °C represented the evaporation of adsorbed water in the inner polymer. The total weight loss was about 10% of the initial weight and this value was almost the same for all heating rates. After the water removal, the main structure started to decompose due to increasing temperature. The curves indicated that the main decomposition zones were in the temperature range of 265-373, 285-380 and 300-400 °C for 5, 10 and 20 °C/min heating rates, respectively. The decomposition related to the deacetylation and depolymerization of the chitosan with the approximately 50% weight loss (Moussout et al. 2016; Moussout et al., 2018). When the DTG curves showing the reaction zone where various reaction steps were occurring over the entire temperature range examined, the maximum peak temperature was determined as 311.2 °C at 5 °C/min heating rate. The increase in the heating rate led to a shift in

maximum peak temperature towards higher value due to the thermal lag. This value was 327.5 and 345.2 °C for 10 and 20 °C/min heating rate. Furthermore, the variation in heating rate affected the completion of the decomposition process. This process completed higher temperature with an incremental rise of the heating rate.

3.2. Kinetic Modelling

The thermal decomposition kinetics of the chitosan could be estimated on a single reaction and can be expressed under isothermal conditions by the following equation:

$$\frac{dx}{dt} = k(T)f(x) = A \exp\left(-\frac{E}{RT}\right)f(x) \quad (1)$$

where t is the time, x depicts the conversion degree, or extent of reaction, dx/dt is the isothermal reaction rate, and $f(x)$ is the conversion function that shows the reaction model used and depends on the controlling mechanisms. The extent of reaction, x , can be defined either as the mass fraction of chitosan that has decomposed as shown below:

$$x = \frac{w_0 - w_t}{w_0 - w_f} \quad (2)$$

where w_0 is the initial mass, w_t is the sample mass present at any time t , w_f is the final mass of sample. The non-isothermal rate expressions as a function of temperature at a linear heating rate, β , can be expressed in Equation 3.

$$\frac{dx}{dT} = \frac{dx}{dt} \frac{dt}{dT} \quad (3)$$

where dt/dT is the inverse of the heating rate, $1/\beta$, dx/dt shows the isothermal reaction rate, and dx/dT is the non-isothermal reaction rate. Thus, an expression of the rate law for non-isothermal conditions can be obtained by substituting Equation (3) into Equation (1):

$$\frac{dx}{dT} = \frac{k(T)f(x)}{\beta} = \frac{A}{\beta} \exp\left(-\frac{E}{RT}\right)f(x) \quad (4)$$

Equation (4) could be integrated in Equation (5)

$$\int_0^x \frac{dx}{f(x)} = g(x) = \frac{A}{\beta} \int_{T_0}^T \exp\left(-\frac{E}{RT}\right) dT = \frac{AE}{\beta R} p(u) \quad (5)$$

where $p(u)$ and $g(x)$ indicate the temperature integral and the integral form of the reaction model, respectively. Relied on the kinetic methods applied, $p(u)$ can be given by many linear approximations. To determine the chitosan kinetics, isoconversional methods can be used without reaction model estimation, $f(x)$. In this method, the value of the activation energy can be calculated at progressive degrees of conversion. Four isoconversional models for calculating activation energy from TG data are used in this study and these models were applied to main decomposition region (Akahira and Sunose, 1971; Starink 1966; Ozawa 1965; Nicolescu et al. 2015). The linear equations of each model are shown in Table 1.

Table 1. Linear equations of FWO, KAS, Starink, and Tang models

Kinetic model	General model equations
FWO	$\ln(\beta) = \ln\left(\frac{AE}{Rg(x)}\right) - 5.331 - 1.052 \frac{E}{R} \frac{1}{T}$
KAS	$\ln\left(\frac{\beta}{T^2}\right) = \ln\left(\frac{AR}{Eg(x)}\right) - \frac{E}{RT}$
Starink	$\ln\left(\frac{\beta}{T^{1.92}}\right) = C - 1.0008 \frac{E}{RT}$
Tang	$\ln\left(\frac{\beta}{T^{1.8947}}\right) = C - 1.0015 \frac{E}{RT}$

By using the slopes of the plots obtained by linear equations of FWO, KAS, Starink, and Tang models, activation energy, the minimum energy requirement for a reaction started, can be calculated for each conversion degree. The typical plots for FWO, KAS, Starink, and Tang models are presented in Figure 2, respectively. As shown in Figure 2, the lines parallel each other and the similar parallelism trend was observed for all studied kinetic models. The parallelism of lines was attributed to the similar kinetic behavior and probably the single reaction mechanism was achieved.

Figure 3 and Table 2 show the activation energy value as a function of conversion degree for different kinetic models. It can be seen that the calculated average activation energy values were close to each other. The average activation energy value was calculated as 148.5, 146.4, 148.3 and 146.7 kJ/mol for FWO, KAS, Starink, and Tang models, respectively. The minor differences in calculated values were attributed to the solution of the integral function by using different approaches. The values for average activation energy calculated using different isoconversional methods were consistent with the previous study found in the literature (Moussout et al. 2016).

As can be seen in Table 2, the high R^2 (>0.98) values were obtained for the studied models. The good correlation coefficient indicated that the calculated activation energy values as a function of conversion degree in the range from 0.1 to 0.9 corresponding model data fitted the experimental data very well. That is, the results obtained were accurate and reliable.

To detect the appropriate reaction models for the thermal decomposition of the chitosan, fifteen different reaction models proposed by the Coats-Redfern method that considered the rate-limiting steps of diffusion, reaction or nucleation were utilized in this study (Ebrahimzad et al. 2017). The reaction mechanism and plotting methods are shown in Table 3.

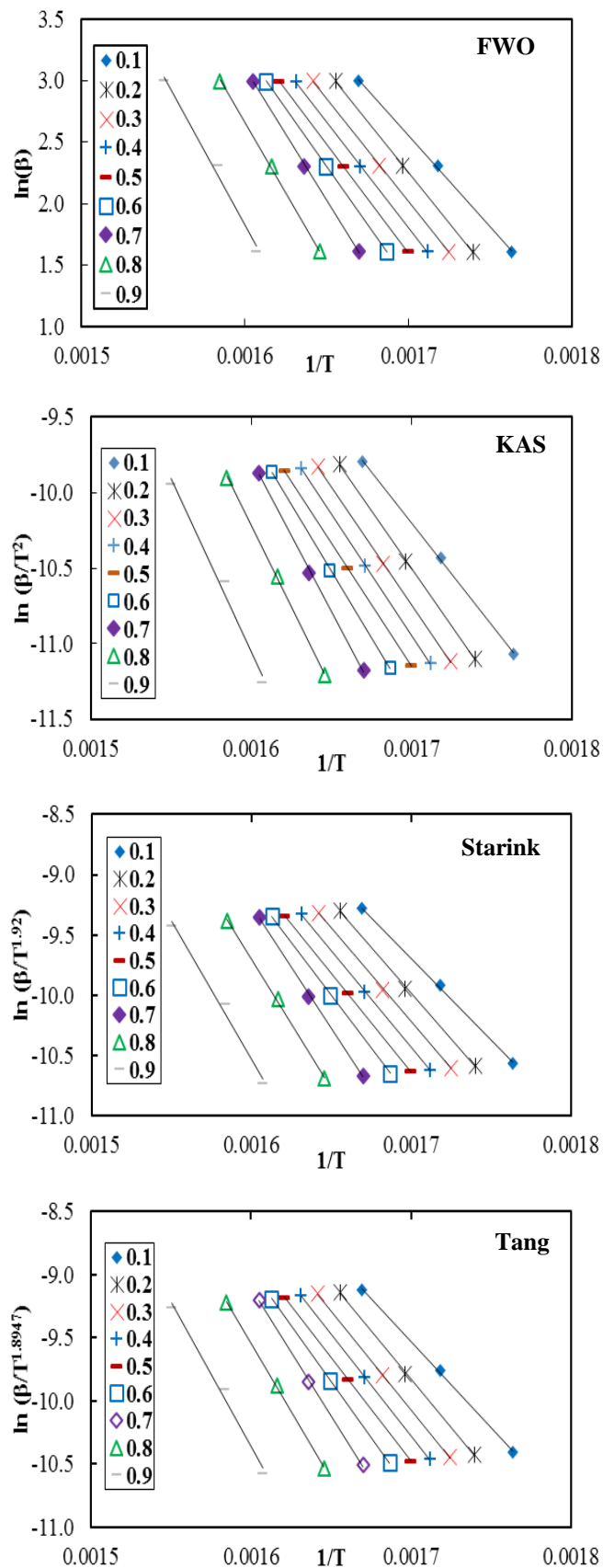
**Figure 2.** Plots for FWO, KAS, Starink, and Tang models

Table 2. The activation energy value according to conversion degree for FWO, KAS, Starink, and Tang models

x	FWO		KAS		Starink		Tang	
	E	R ²	E	R ²	E	R ²	E	R ²
0.1	112.1	0.9972	112.8	0.9990	125.0	0.9990	108.7	0.9993
0.2	129.6	0.9996	126.7	0.9997	126.9	0.9997	127.2	0.9990
0.3	132.4	0.9999	129.5	0.9999	129.8	0.9999	130.0	0.9994
0.4	135.9	0.9984	133.1	0.9999	133.4	0.9995	133.7	0.9988
0.5	138.5	0.9999	133.1	0.9992	136.0	0.9999	136.2	0.9989
0.6	148.3	0.9999	146.0	0.9991	146.2	0.9996	146.5	0.9991
0.7	168.6	0.9992	167.2	0.9998	167.4	0.9992	167.7	0.9991
0.8	180.0	0.9994	179.1	0.9993	179.4	0.9993	180.2	0.9990
0.9	190.4	0.9903	190.0	0.9891	190.3	0.9892	190.6	0.9988
Average	148.5		146.4		148.3		146.7	

The plots for various diffusion, nucleation, reaction order and geometric contraction models for 10 °C/min are given in Figure 4. The reaction mechanism applications were numbered according to the Table 3. The linear fitting was not obtained for diffusion controlled and nucleation reaction models.

The correlation coefficients, R², which are the criteria of how much the calculated model values and TG values match, are presented in Table 4. After examining the Table 4, it can be concluded that the reaction order model was the best model to statistically characterize the TG data and the highest R² values were provided for the second reaction order for all studied heating rates.

Table 3. Kinetic integration functions g(x) for different reaction mechanisms

No	Reaction mechanism	g(x)
Diffusion models		
1	One-dimensional diffusion	x ²
2	Two-dimensional diffusion (Valensi)	x+[(1-x)ln(1-x)]
3	Three-dimensional diffusion (Jander)	[1-(1-x) ^{1/3}] ²
4	Anti-Jander equation	[(1+x) ^{1/3} -1] ²
5	Three-dimensional diffusion (Ginstling-Brounstein)	1-(2/3)x-(1-x) ^{2/3}
Nucleation models		
6	Power law	x
7	Power law	x ^{1/2}
8	Power law	x ^{1/3}
9-11	n= 2, 3, 4 (Avrami-Erofeev)	[-ln(1-x)] ^{1/n}
Reaction order and geometric contraction models		
12	First-order (Mampel)	-ln(1-x)
13	Reaction order (n=2)	[(1-x) ⁽¹⁻ⁿ⁾ -1]/(n-1)
14	Contraction of cylinder	1-(1-x) ^{1/2}
15	Contraction of sphere	1-(1-x) ^{1/3}

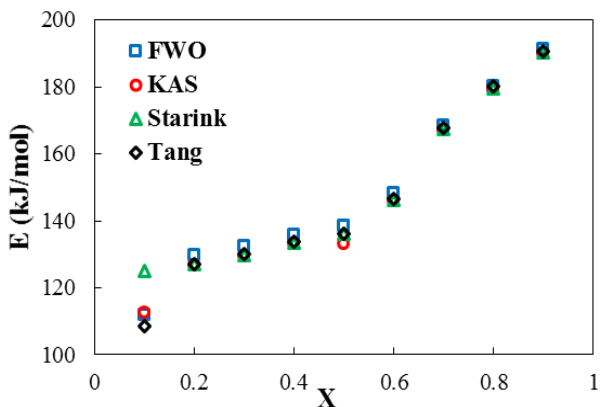


Figure 3. Calculated activation energy value with respect to conversion degree

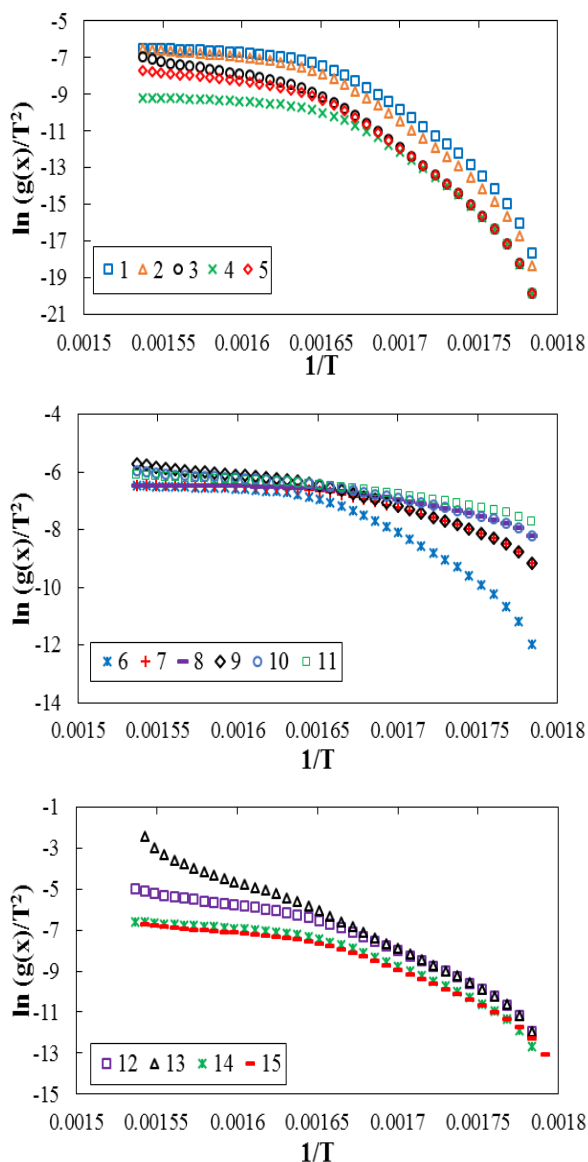


Figure 4. Variation models of chitosan for 10 °C/min heating rate

4. Conclusions

In this study, thermal decomposition experiments of chitosan were conducted in an inert N₂ atmosphere by means of a thermogravimetric analyzer. With the obtained TGA data, kinetic analysis was carried out, besides thermal behaviors of chitosan at different heating rates were investigated. FWO, KAS, Starink, and Tang kinetic models were utilized to calculate the activation energy. The average activation values were determined as 148.5, 146.4, 148.3 and 146.7 kJ/mol for FWO, KAS, Starink and Tang models, respectively. All models used provided accurate fits of each other with high R² values. In addition, it was determined that the second reaction order model was the best one to characterize the results among the other studied models.

Table 4. R² values for different reaction mechanisms

No	5 °C/min	10 °C/min	20°C/min
Diffusion controlled models			
1	0.8026	0.8321	0.8382
2	0.8337	0.8599	0.8651
3	0.8758	0.8968	0.9007
4	0.7821	0.8143	0.8209
5	0.8482	0.8727	0.8775
Nucleation reaction models			
6	0.7793	0.8274	0.8214
7	0.7202	0.8175	0.7800
8	0.6390	0.8068	0.7246
9	0.8836	0.9246	0.9123
10	0.8542	0.9208	0.8938
11	0.8132	0.9167	0.8694
Reaction order and geometric contraction models			
12	0.9053	0.9281	0.9264
13	0.9814	0.9879	0.9955
14	0.8471	0.8768	0.8622
15	0.8692	0.9032	0.8902

References

Akahira T, Sunose T 1971. Method of determining activation deterioration constant of electrical insulating materials. Res. Rep. Chiba Inst. Technol (Sci Technol) 16: 22-31.

Ebrahimzad H, Khayati GR, Schaffie M 2017. Preparation and kinetic modeling of β-Co(OH)₂ nanoplates thermal decomposition obtained from spent Li-ion batteries. Adv Powder Technol 28: 2779-2786.

- Flynn JH, Wall LA 1966. General treatment of the thermogravimetry of polymers. *J. Res. Nat. Bur. Stand* 70: 487-523.
- Hamed H, Moradi S, Hudson SM, Tonelli AE 2018 Chitosan based hydrogels and their applications for drug delivery in wound dressings: A review. *Carbohydrate Polymers* 199: 445-460.
- Kast CE, Valenta C, Leopold M, Bernkop-Schnürch A 2002. Design and in vitro evaluation of a novel bioadhesive vaginal drug delivery system for clotrimazole. *Journal of Controlled Release* 81: 347-354.
- Lozano-Navarro JI, Díaz-Zavala NP, Velasco-Santos C, Melo-Banda JA, Páramo-García U, Paraguay-Delgado F, García-Alamilla R, Martínez-Hernández AL, Zapién-Castillo S 2018 Chitosan-Starch Films with Natural Extracts: Physical, Chemical, Morphological and Thermal Properties. *Materials* 11: 120.
- Moussout H, Ahlafi H, Aazza M, Bourakhouadar M 2016. Kinetics and mechanism of the thermal degradation of biopolymers chitin and chitosan using thermogravimetric analysis. *Polymer Degradation and Stability* 130: 1-9.
- Moussout H, Ahlafi H, Aazza M, Bourakhouadar M, Amechrouq A 2018. Bentonite/chitosan nanocomposite: Preparation, characterization and kinetic study of its thermal degradation. *Thermochimica Acta* 659: 191-202.
- Nicolescu LC, Tita B, Jurca T, Marian E, Tita D 2015. Thermal Stability of Piroxicam – Active Substance and Tablets. I. Kinetic study of the active substance under nonisothermal conditions. *Rev. Chim.-Bucharest* 66: 1802-1806.
- Ozawa T 1965. A new method of analyzing thermogravimetric data. *Bulletin Chem. Soc. Japan* 38: 1881-1886.
- Starink M 1966. A new method for the derivation of activation energies from experiments performed at constant heating rate. *Thermochimica Acta* 288: 97-104.
- Qu X, Wirsén A, Albertsson C 2000. Effect of lactic/glycolic acid side chains on the thermal degradation kinetics of chitosan derivatives. *Polymer* 41: 4841-4847.
- Zhou L, Wang Y, Liu Z, Huang Q 2009. Characteristics of equilibrium, kinetics studies for adsorption of Hg(II), Cu(II), and Ni(II) ions by thiourea-modified magnetic chitosan microspheres. *Journal of Hazardous Materials* 161: 995-1002.